

Negative quantum Hall effect in field-induced spin-density-wave states: Dependence on shape of the quasi-one-dimensional Fermi surface

Keita Kishigi

Faculty of Education, Kumamoto University, Kurokami 2-40-1, Kumamoto 860-8555, Japan

Yasumasa Hasegawa

Department of Material Science, Graduate School of Material Science, University of Hyogo, Hyogo 678-1297, Japan

(Received 11 May 2009; published 25 August 2009)

The successive transitions of the field-induced spin-density wave, which is labeled by the quantum number N of the Hall conductivity and the nesting vector, are known to depend on the shape of the quasi-one-dimensional Fermi surface. We study the condition for the appearance of the negative N states, where the quantized Hall conductivity changes the sign. We obtain the phase diagram for the negative N states in the parameter space of the higher harmonics in the Fermi surface (t'_b , t_3 , and t_4) to be stabilized with and without the periodic anion potential V in the perpendicular direction to the conducting axis, which are the cases in (TMTSF)₂ClO₄ and (TMTSF)₂PF₆, respectively. The negative N phase is shown to be stabilized for the smaller values of t_3 and t_4 in the case of the finite V . Comparing with the experiment by Matsunaga *et al.* [J. Phys. IV **131**, 269 (2005)], where the quantum Hall effect is observed in (TMTSF)₂ClO₄ with various cooling rates, we obtain the parameter regions of t_3 and t_4 for (TMTSF)₂ClO₄ ($0.06 \leq t_3/t'_b \leq 0.23$, $0 \leq t_4/t'_b \leq 0.08$, and $V/t'_b \leq 2.0$).

DOI: [10.1103/PhysRevB.80.075119](https://doi.org/10.1103/PhysRevB.80.075119)

PACS number(s): 78.30.Jw, 75.30.Fv, 73.43.-f

I. INTRODUCTION

In the organic conductors (TMTSF)₂X ($X = \text{ClO}_4$, PF₆, etc.) many interesting phenomena such as the field-induced spin-density wave (FISDW),¹⁻⁷ the quantum Hall effect and the negative Hall resistance (R_{xy}) in some regions of the magnetic field [$X = \text{ClO}_4$,⁷⁻⁹ PF₆,¹⁰⁻¹² ReO₄,¹³ and AsF₆ (Ref. 14)], superconductivity,^{15,16} and anomalous peak structures of the angular-dependent magnetoresistance¹⁷ have been observed. These organic conductors have the quasi-one-dimensional Fermi surface. The simplest model may be the 3/4-filled tight-binding model (or 1/4 filled with holes)

$$\epsilon_0(\mathbf{k}) = -2t_a \cos(ak_x) - 2t_b \cos(bk_y), \quad (1)$$

where a and b are the lattice constants along x and y axes, respectively, and t_a and t_b are the anisotropic transfer integrals which are roughly obtained from experiments as $\{t_a, t_b\} \simeq \{258 \text{ meV}, 25.4 \text{ meV}\}$ for ClO₄ and $\{t_a, t_b\} \simeq \{264 \text{ meV}, 23.4 \text{ meV}\}$ for PF₆.^{1,18} The transfer integral along the third direction (t_c) is about $t_b/10$ and it can be neglected.^{1,18} Although the crystal is triclinic and there are the multiple-transverse-transfer integrals,¹⁸⁻²⁰ most of the important properties are understood by Eq. (1).¹

Equation (1) is further simplified by linearizing the energy with respect to k_x including the higher harmonics of k_y

$$\epsilon(\mathbf{k}) = \hbar v_F (|k_x| - k_F) + t_\perp(k_y), \quad (2)$$

where

$$t_\perp(k_y) = -2t_b \cos(bk_y) - 2t'_b \cos(2bk_y) - 2t_3 \cos(3bk_y) - 2t_4 \cos(4bk_y) - 2t_5 \cos(5bk_y) - \dots, \quad (3)$$

$$t_a \gg t_b \gg t'_b \gg t_3 \gg t_4 \gg t_5 \gg \dots, \quad (4)$$

$v_F = \frac{\sqrt{2}at_a}{\hbar}$, and $k_F = \frac{\pi}{4a}$. Hereafter, we set $\hbar = 1$. By using the perturbation with respect to t_b/t_a in Eq. (1), we get $t'_b \sim O[(\frac{t_b}{t_a})^2]$, $t_n \sim O[(\frac{t_b}{t_a})^n]$, and ($n = 3, 4, \dots$). The parameter (t'_b) gives the imperfectness of the nesting of the quasi-one-dimensional Fermi surface with the nesting vector

$$\mathbf{Q}_0 = \left(2k_F, \frac{\pi}{b} \right) \quad (5)$$

and is the origin of the FISDW. Therefore, we scale the other parameters by t'_b . In this paper we set $t_a/t'_b = 100$ and $t_b/t'_b = 10$, where t_a , t_b , and t'_b are taken to be positive. It has been known that a small change in the Fermi surface due to t_3 and t_4 plays an important role of the presence of the negative Hall effect^{21,22} and the superconductivity.²³ In the tight-binding model with single-transverse-transfer integral [Eq. (1)], t_n ($n = 3, 4, \dots$) is obtained in terms of t_a and t_b by perturbation from Eq. (1) as mentioned above. However, in general, there are multiple-transverse-transfer integrals and t_3 , t_4 , etc., depend on these transfer integrals by perturbation. Therefore, as we cannot take t_3 and t_4 as the parameters depending on t_a and t_b , we consider these as the independent parameters. We ignore the higher terms (t_5, \dots) since these do not play an important role for the FISDW state.

The FISDW states are labeled by an integer N of the spin-density wave (SDW) number $Q_x = 2k_F + NG$, where $G = beB$ and B is the magnetic field.²⁴⁻³³ It has been shown that the quantization of the Hall effect is characterized by the quantum number N of the FISDW wave vector³⁴⁻³⁶ and the sign change has been explained by multi-SDW order parameter³⁷ and t_3 and t_4 .^{21,22} These higher terms are also used in the study of the magnetoroton modes.³⁸

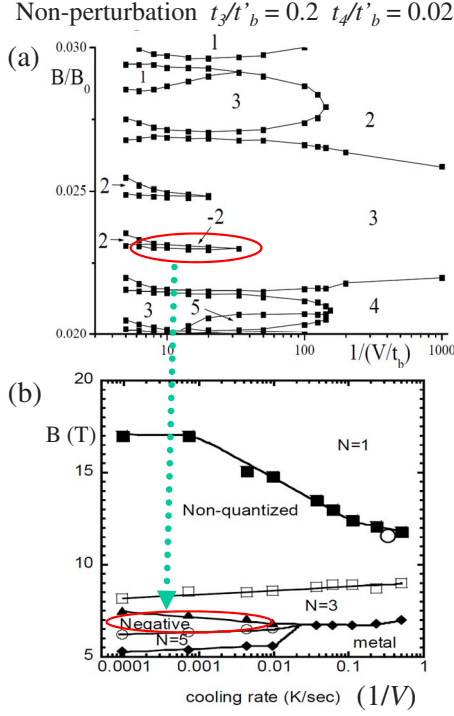


FIG. 1. (Color online) (a) The $1/V$ and B phase diagram obtained by nonperturbation (Ref. 47). (b) Cooling rate dependence of the FISDW phase diagram in deuterated $(\text{TMTSF})_2\text{ClO}_4$ at 0.5 K (Ref. 45).

The shape of the Fermi surface is also affected by the anion ordering at $T_{\text{AO}}=24$ K in $(\text{TMTSF})_2\text{ClO}_4$. Interesting properties have been reported in the magnetic field, i.e., the superconducting critical temperature with the anomalous in-plane anisotropy,^{39,40} which is attributed to the Fulde-Ferrel-Larkin-Ovchinnikov (FFLO) state,^{41,42} the unclosed anomalous FISDW first-order transition line in the B —temperature (T) phase diagram,^{43–45} the periodic oscillation⁴⁶ with sign reversal of R_{xy} above $B \approx 26$ T, etc. The alternating ordering of the anion ClO_4 in the y direction below $T_{\text{AO}}=24$ K is thought to cause these phenomena. The ordering of the anion gives the periodic potential with the wave vector $\mathbf{Q}_A = (0, \pi/b)$. Then the Hamiltonian is written as a 2×2 matrix,

$$\hat{\mathcal{H}} = \hat{\mathcal{H}}_0 + \hat{\mathcal{H}}_V = \begin{pmatrix} \epsilon(\mathbf{k}) & V \\ V & \epsilon(\mathbf{k} + \mathbf{Q}_A) \end{pmatrix}, \quad (6)$$

where V is the magnitude of the periodic potential and we set $V \geq 0$. The eigenvalues (ϵ^\pm) are obtained as

$$\epsilon^\pm(\mathbf{k}) = \frac{1}{2} \{ [\epsilon(\mathbf{k}) + \epsilon(\mathbf{k} + \mathbf{Q}_A)] \pm \sqrt{[\epsilon(\mathbf{k}) - \epsilon(\mathbf{k} + \mathbf{Q}_A)]^2 + 4V^2} \}, \quad (7)$$

which gives two pairs of open sheetlike Fermi surfaces.

In the previous paper, we have obtained the phase diagram of the FISDW in the plane of the inverse of the potential V and B as shown in Fig. 1(a). In that case we have used the parameter $t_3/t'_b=0.2$ and $t_4/t'_b=0.02$. The strength of the potential V is thought to be controlled experimentally by

changing the cooling rate. If the sample is cooled very slowly, the anion orders completely and the potential V is large. If the cooling rate is larger but still it makes anions order, the ordering occurs partially and V is smaller. With this interpretation we have compared our results with experiments by Matsunaga *et al.*,⁴⁵ who have observed the Hall resistance in the condition of various cooling rates and magnetic field. The observed phase diagram is shown as in Fig. 1(b). The appearance of the negative phase is reproduced by the $N=-2$ phase in the calculation, as marked by the red obliques in Figs. 1(a) and 1(b). The $N=-2$ phase appears in the intermediate values of V ($7 \lesssim t_b/V \lesssim 30$, i.e., $0.3 \lesssim V/t'_b \lesssim 1.5$). This is consistent with the upper limit for V ,

$$V < 2t'_b - 2t_4, \quad (8)$$

which is obtained from the susceptibility for $B=0$.⁴⁸ Since the $N=-2$ phase is observed in the slowest cooling rate, we can conclude that V in $(\text{TMTSF})_2\text{ClO}_4$ should be smaller than $2t'_b - 2t_4$. The estimated value of V from the angular dependence of the magnetoresistance by Lebed *et al.*⁴⁹ ($V \sim 2.0t'_b$) is close to the boundary, while the value estimated by Yoshino *et al.*⁵⁰ ($V \sim 3.36t'_b$) is larger than our estimation.

The extensive study for the possible values for t_3 , t_4 , and V has not been done as far as we know. These parameters change the shape of the Fermi surface slightly when $t_4 \ll t_3 \ll t'_b$ but they cause the difference in the FISDW state, especially concerning to the negative N phase. In this paper we give the parameter regions for t_3 and t_4 in which the negative phase is stabilized in some regions of the magnetic field in $V=0$ and in a finite value of V .

II. SUSCEPTIBILITY IN THE MAGNETIC FIELD

The effect of the magnetic field is studied by the substitution,

$$k_x = -i \frac{\partial}{\partial x}, \quad (9)$$

$$k_y = -i \frac{\partial}{\partial y} + Gx \quad (10)$$

in Eq. (6). The spin splitting due to the Zeeman effect is not taken into account since that effect is not important in the transverse susceptibility, although it plays a crucial role in the case of charge-density wave (CDW). In this study, we take $0 \leq V/t'_b \leq 2.0$, $0 \leq t_3/t'_b \leq 0.3$, and $0 \leq t_4/t'_b \leq 0.125$. Zanchi and Montambaux²¹ have employed $t_a/t'_b=300$, $t_b/t'_b=30$, $t_3/t'_b=0.07$, $t_4/t'_b=0.0025$, and $k_B T/t'_b=0.05$. Lederer and Chaves³⁸ have used $t_a/t'_b=300$, $t_b/t'_b=26.5$, $0.03 \leq t_3/t'_b \leq 0.07$, and $0.0025 \leq t_4/t'_b \leq 0.03$.

A. Susceptibility in the magnetic fields without the anion ordering

The susceptibility in the quasi-one-dimensional systems in the magnetic field has been studied by many authors^{24–33} when the periodic potential is zero. Here, we give the results

including t_3 and t_4 terms. The eigenstates of the quasi-one-dimensional electrons are given as

$$|(\mathbf{K} + n\mathbf{G})^l\rangle = \exp \left[i \left\{ (-k_F + K_x + nG)x + K_y y + \frac{1}{v_F G} \int_0^{bK_y + Gx} t_\perp(p) dp \right\} \right] \quad (11)$$

and

$$|(\mathbf{K} + n\mathbf{G})^r\rangle = \exp \left[i \left\{ (k_F + K_x + nG)x + K_y y - \frac{1}{v_F G} \int_0^{bK_y + Gx} t_\perp(p) dp \right\} \right] \quad (12)$$

for the left and the right parts of the Fermi surface, respectively, where $\mathbf{G} = (G, 0) = (beB, 0)$ and $0 \leq K_x \leq G$. The eigenvalues for these states are

$$E_{\mathbf{K}+n\mathbf{G}}^l = -v_F(K_x + nG),$$

$$E_{\mathbf{K}+n\mathbf{G}}^r = v_F(K_x + nG),$$

respectively. The susceptibility for the noninteracting system in the magnetic field is given by

$$\begin{aligned} \tilde{\chi}_{00}(\mathbf{Q}, B) &= \frac{1}{\Omega} \sum_{n, n'} \sum_{\mathbf{K}, \mathbf{K}'} | \langle (\mathbf{K}' + n'\mathbf{G} + \mathbf{Q} - 2\mathbf{k}_F)^r | e^{i\mathbf{Q}\cdot\mathbf{r}} | (\mathbf{K} + n\mathbf{G})^l \rangle |^2 \\ &\times \frac{f(E_{\mathbf{K}+n\mathbf{G}}^l) - f(E_{\mathbf{K}'+n'\mathbf{G}+\mathbf{Q}-2\mathbf{k}_F}^r)}{E_{\mathbf{K}'+n'\mathbf{G}+\mathbf{Q}-2\mathbf{k}_F}^r - E_{\mathbf{K}+n\mathbf{G}}^l}, \end{aligned} \quad (13)$$

where Ω is the volume of the system and $\mathbf{k}_F = (k_F, 0)$. The matrix element is given by

$$\begin{aligned} &| \langle (\mathbf{K}' + n'\mathbf{G} + \mathbf{Q} - 2\mathbf{k}_F)^r | e^{i\mathbf{Q}\cdot\mathbf{r}} | (\mathbf{K} + n\mathbf{G})^l \rangle | \\ &= \delta_{K_x, K'_x} e^{i(n-n')(bK_y + bQ_y/2)} I_{n-n'}(Q_y), \end{aligned} \quad (14)$$

where

$$\begin{aligned} I_{n-n'}(Q_y) &= \int_0^{2\pi} \frac{dp}{2\pi} \exp \left[i \left\{ (n-n')p - \frac{1}{v_F G} \times \left[\int_0^{p+bQ_y/2} t_\perp(p') dp' + \int_0^{p-bQ_y/2} t_\perp(p') dp' \right] \right\} \right] \\ &= (-1)^{n-n'} \sum_{l=-\infty}^{\infty} \sum_{l'=-\infty}^{\infty} \sum_{l''=-\infty}^{\infty} (-1)^l (-1)^{l'} J_{n-n'-2l-3l'-4l''} \left[\frac{4t_b \cos(bQ_y/2)}{v_F G} \right] J_l \left[\frac{2t'_b \cos(bQ_y)}{v_F G} \right] \\ &\times J_{l'} \left[\frac{4t_3 \cos(3bQ_y/2)}{3v_F G} \right] J_{l''} \left[\frac{t_4 \cos(2bQ_y)}{v_F G} \right] \end{aligned} \quad (15)$$

and J_l is the Bessel function of the first kind.

As a result, the susceptibility is written as

$$\tilde{\chi}_{00}(\mathbf{Q}, B) = \sum_N |I_N(Q_y)|^2 \chi_0^{1D}(Q_x + NG), \quad (16)$$

where $\chi_0^{1D}(Q_x)$ is the susceptibility for the one-dimensional system given by

$$\begin{aligned} \chi_0^{1D}(Q_x) &= \sum_{K_x} \sum_n \frac{f(E_{K_x+nG}^l) - f(E_{K_x+nG+Q_x-2k_F}^r)}{E_{K_x+nG+Q_x-2k_F}^r - E_{K_x+nG}^l}, \\ &\simeq N(0) \int_{-\xi_c}^{\xi_c} d\xi \frac{f(-\xi + \varepsilon_{Q_x}) - f(\xi + \varepsilon_{Q_x})}{2\xi}, \end{aligned} \quad (17)$$

where $\varepsilon_{Q_x} = v_F(Q_x - 2k_F)/2$, ξ_c is a cut-off energy on the order of t_a , and $N(0)$ is the density of states at Fermi energy.

While it has a sharp cusplike maximum with respect to Q_x at $Q_x = 2k_F + NG$, the maximum with respect to Q_y is broad.

B. Susceptibility in the magnetic fields with the anion ordering

When the anions order and give the periodic potential V , the eigenstates and the susceptibility become complicated.^{47,48,51-60} The noninteracting susceptibility is a 2×2 matrix^{56-58,60} in the presence of V because there are two nonequivalent sites in the unit cell or the two bands. The off-diagonal components of the susceptibility, however, are very small in the parameter region studied in this paper, i.e., $-1 \leq v_F q_x / t_b \leq 1$ and $q_y \approx 0$ at small V ($0 \leq V/t_b' \leq 0.2$) and in the weak field ($7 \text{ T} \leq B \leq 12 \text{ T}$). Therefore, we neglect the off-diagonal elements and study only the diagonal elements of the susceptibility.

We give the results^{47,51-54} including V in addition to t_3 and t_4 terms in this section. The eigenstates for the left and right parts of the Fermi surfaces are expressed as the linear combinations of the eigenstates for $V=0$ as

$$|\Psi_n^{l(r)(\pm)}(\mathbf{K})\rangle = \sum_m v_{mn}^{l(r)(\pm)} |(\mathbf{K} + m\mathbf{G})^{l(r)(\pm)}\rangle, \quad (18)$$

where

$$|(\mathbf{K} + m\mathbf{G})^{l(r)(\pm)}\rangle = \frac{1}{\sqrt{2}} e^{imbK_y} \{ |(\mathbf{K} + m\mathbf{G})^{l(r)}\rangle \pm (-1)^m |(\mathbf{K} + m\mathbf{G} + \mathbf{Q}_A)^{l(r)}\rangle \}. \quad (19)$$

By taking $|(\mathbf{K} + m\mathbf{G})^{l(r)(\pm)}\rangle$ as the basis set, we obtain the matrix elements of $\mathcal{H}_0 + \mathcal{H}_V$ as followings:

$$(\mathcal{H}_0)_{mn}^{l(\pm)} = \langle (\mathbf{K} + m\mathbf{G})^{l(\pm)} | \mathcal{H}_0 | (\mathbf{K} + n\mathbf{G})^{l(\pm)} \rangle = -\delta_{m,n} v_F (K_x + nG), \quad (20)$$

$$(\mathcal{H}_0)_{mn}^{r(\pm)} = \langle (\mathbf{K} + m\mathbf{G})^{r(\pm)} | \mathcal{H}_0 | (\mathbf{K} + n\mathbf{G})^{r(\pm)} \rangle = \delta_{m,n} v_F (K_x + nG), \quad (21)$$

$$(\mathcal{H}_v)_{mn}^{l(\pm)} = \langle (\mathbf{K} + m\mathbf{G})^{l(\pm)} | \mathcal{H}_v | (\mathbf{K} + n\mathbf{G})^{l(\pm)} \rangle = (-1)^n V \sum_{l=-\infty}^{\infty} J_{m-n-3l} \left(\frac{4t_b}{v_F G} \right) J_l \left(\frac{4t_3}{3v_F G} \right), \quad (22)$$

$$(\mathcal{H}_v)_{mn}^{r(\pm)} = \langle (\mathbf{K} + m\mathbf{G})^{r(\pm)} | \mathcal{H}_v | (\mathbf{K} + n\mathbf{G})^{r(\pm)} \rangle = (-1)^m V \sum_{l=-\infty}^{\infty} J_{m-n-3l} \left(\frac{4t_b}{v_F G} \right) J_l \left(\frac{4t_3}{3v_F G} \right). \quad (23)$$

By diagonalizing Hamiltonian (20)–(23) numerically, the coefficients $v_{mn}^{l(r)(\pm)}$ in Eq. (18) are obtained. The eigenvalues for the left and right Fermi surface are

$$E_{K_x+nG}^{l(\pm)} = -v_F (K_x + nG) \pm (-1)^n \Delta, \quad (24)$$

$$E_{K_x+nG}^{r(\pm)} = v_F (K_x + nG) \pm (-1)^n \Delta, \quad (25)$$

where Δ is the splitting of the energy band. When V is very small or the magnetic field is extremely large, Δ is written in terms of the Bessel function.^{61–64} In general case, however, it should be obtained numerically.

The susceptibility in the magnetic field is described in terms of the eigenstates as

$$\begin{aligned} \tilde{\chi}_0(\mathbf{Q}, B) &= \left| \sum_{n,n'} \sum_{\mathbf{K}} \sum_{\gamma,\gamma'=\pm} \langle \Psi_n^{r(\gamma')}(\mathbf{K} + \mathbf{Q} - 2\mathbf{k}_F) | e^{i\mathbf{Q}\cdot\mathbf{r}} | \Psi_n^{l(\gamma)}(\mathbf{K}) \rangle \right|^2 \\ &\times \frac{f(E_{K_x+nG}^{l(\gamma)}) - f(E_{K_x+Q_x-2k_F+n'G}^{r(\gamma')})}{E_{K_x+Q_x-2k_F+n'G}^{r(\gamma')} - E_{K_x+nG}^{l(\gamma)}}. \end{aligned} \quad (26)$$

Finally, the susceptibility is given by⁵³

$$\begin{aligned} \tilde{\chi}_0(\mathbf{Q}, B) &= \sum_n \{ |A_{2n}^{++}(Q_y)|^2 \tilde{\chi}_0^{++}(Q_x - 2k_F + 2nG) \\ &+ |A_{2n}^{--}(Q_y)|^2 \tilde{\chi}_0^{--}(Q_x - 2k_F + 2nG) + [|A_{2n}^{+-}(Q_y)|^2 \\ &+ |A_{2n}^{-+}(Q_y)|^2] \tilde{\chi}_0^{+-}[Q_x - 2k_F + (2n+1)G] \}, \end{aligned} \quad (27)$$

where

$$A_{2n}^{++}(Q_y) = \sum_{m,m'} v_{m'0}^{r(+)*} v_{-m0}^{r(+)} e^{i(m-m')bQ_y/2} \times I_{m-m'+2n}(Q_y), \quad (28)$$

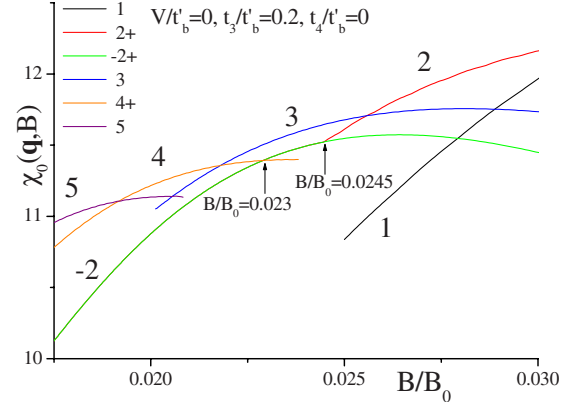


FIG. 2. (Color online) The maximum of $\chi_0(\mathbf{q}, B)$ for the non-perturbative calculation for $V/t'_b=0$ and $t_3/t'_b=0.2$, $t_4/t'_b=0$.

$$A_{2n}^{--}(Q_y) = \sum_{m,m'} (-1)^{m+m'} v_{-m'0}^{r(+)*} v_{m0}^{r(+)} e^{i(m-m')bQ_y/2} \times I_{m-m'+2n}(Q_y), \quad (29)$$

$$A_{2n+1}^{+-}(Q_y) = \sum_{m,m'} (-1)^m v_{m'0}^{r(+)*} v_{m0}^{r(+)} e^{i(m-m')bQ_y/2} \times I_{m-m'+2n+1}(Q_y), \quad (30)$$

$$A_{2n+1}^{-+}(Q_y) = \sum_{m,m'} (-1)^{m'} v_{-m'0}^{r(+)*} v_{-m0}^{r(+)} e^{i(m-m')bQ_y/2} \times I_{m-m'+2n+1}(Q_y) \quad (31)$$

and

$$\tilde{\chi}_0^{++}(Q_x) \approx N(0) \int_{-\xi_c}^{\xi_c} d\xi \times \frac{f(-\xi + \varepsilon_{Q_x} + \Delta) - f(\xi + \varepsilon_{Q_x} + \Delta)}{2\xi}, \quad (32)$$

$$\tilde{\chi}_0^{--}(Q_x) \approx N(0) \int_{-\xi_c}^{\xi_c} d\xi \times \frac{f(-\xi + \varepsilon_{Q_x} - \Delta) - f(\xi + \varepsilon_{Q_x} - \Delta)}{2\xi}, \quad (33)$$

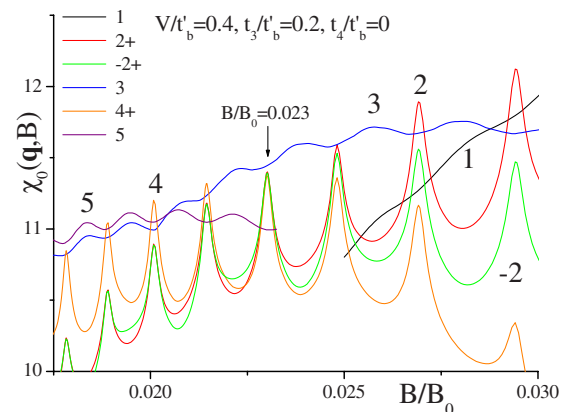


FIG. 3. (Color online) The maximum of $\chi_0(\mathbf{q}, B)$ for the non-perturbative calculation for $V/t'_b=0.4$ and $t_3/t'_b=0.2$, $t_4/t'_b=0$.

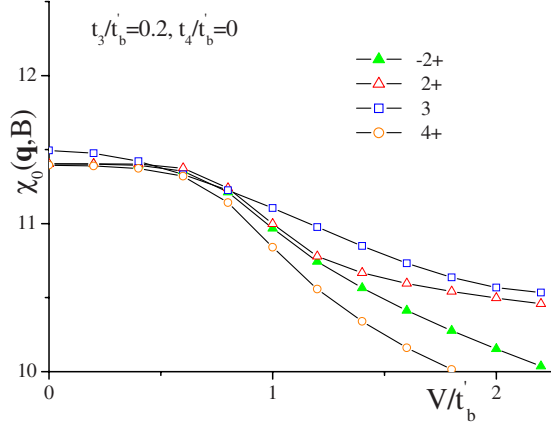


FIG. 4. (Color online) The maximum of $\chi_0(\mathbf{q}, B)$ at $B/B_0 = 0.023$ as a function of V/t'_b .

$$\tilde{\chi}_0^{+-}(\mathcal{Q}_x) \approx N(0) \int_{-\xi_c}^{\xi_c} d\xi \frac{f(-\xi + \varepsilon_{\mathcal{Q}_x}) - f(\xi + \varepsilon_{\mathcal{Q}_x})}{2\xi}. \quad (34)$$

We use \mathbf{q} as the FISDW nesting vector, where $\mathbf{q} = \mathbf{Q} - \mathbf{Q}_0$. Thus,

$$\mathbf{q} = (q_x, q_y) = \left(\mathcal{Q}_x - 2k_F, \mathcal{Q}_y - \frac{\pi}{b} \right). \quad (35)$$

Hereafter, we use $\chi_0(\mathbf{q}, B)$ instead of $\tilde{\chi}_0(\mathbf{Q}, B)$ in Eq. (27) with the definition

$$\chi_0(\mathbf{q}, B) = \tilde{\chi}_0(\mathbf{Q}, B) = \tilde{\chi}_0(\mathbf{q} + \mathbf{Q}_0, B). \quad (36)$$

III. RESULTS AND DISCUSSIONS

The local maximum values of the susceptibility are calculated numerically as a function of B . There are sharp maximums at $q_x = NG$ when N is odd and $q_x = NG \pm 2\Delta/v_F$ when N is even.^{53,63} We label the maximums as N and $N\pm$ for odd and even N , respectively, where q_y is scanned to give the local maximum. We plot the maximum values for N , $N+$, and $N-$ as a function of B/B_0 for $t_3/t'_b = 0.2$, $t_4/t'_b = 0$, and $V/t'_b = 0$ in Fig. 2, where $B_0 = \frac{4t_b}{v_F b e}$. The maximum values for N ,

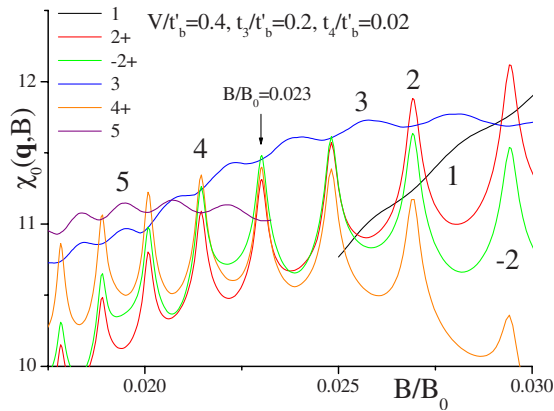


FIG. 5. (Color online) The maximum of $\chi_0(\mathbf{q}, B)$ for the non-perturbative calculation for $V/t'_b = 0.4$ and $t_3/t'_b = 0.2$, $t_4/t'_b = 0.02$.

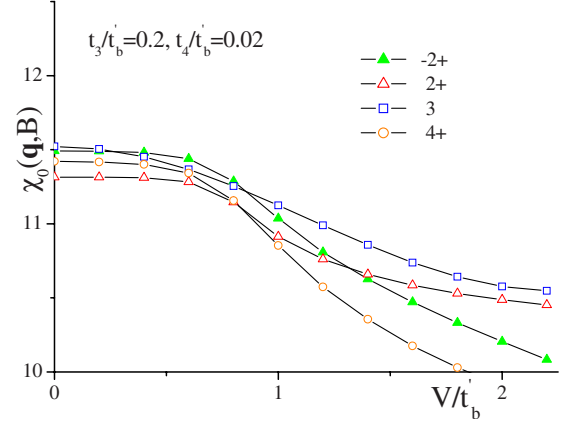


FIG. 6. (Color online) The maximum of $\chi_0(\mathbf{q}, B)$ at $B/B_0 = 0.023$ as a function of V/t'_b .

$N+$, and $N-$ with the same parameters except $V/t'_b = 0.4$ are shown in Fig. 3. When we use $a = b = 0.7$ nm based on the lattice constants of $(\text{TMTSF})_2\text{ClO}_4$ and $(\text{TMTSF})_2\text{PF}_6$, we get $B_0 \approx 400$ T. Thus, $0.0175 \leq B/B_0 \leq 0.03$ and $B/B_0 = 0.023$ are corresponding to $7 \text{ T} \leq B \leq 12 \text{ T}$ and $B \approx 9 \text{ T}$, respectively.

When $V = 0$ and t_3 and t_4 are small, the absolute maximum of $\chi_0(\mathbf{q}, B)$ for each B is given by $N = \dots, 5, 4, 3, 2, \dots$ as B increases (as seen in Fig. 2), which corresponds to the successive transitions between different FISDW phases ($N = \dots, 5, 4, 3, 2, \dots$) with increasing magnetic field. When V is finite, the maximum of $\chi_0(\mathbf{q}, B)$ oscillates as a function of B (see Fig. 3). The amplitudes of the oscillation is small for odd N , if V is small. This is consistent with the perturbation in V in which $\chi_0(\mathbf{q}, B)$ oscillates only for the even N .

Although the maximum of $\chi_0(\mathbf{q}, B)$ for $N = -2$ is smaller than the maximums for $N > 0$ in that choice of the parameters ($t_3/t'_b = 0.2$ and $t_4/t'_b = 0$, see Fig. 2), the maximum of $\chi_0(\mathbf{q}, B)$ for $N = -2+$, $2+$, 3 , and $4+$ at $B/B_0 \approx 0.023$ have almost the same value in $0 \leq V/t'_b \leq 0.4$, which can be seen in Fig. 3. We plot $\chi_0(\mathbf{q}, B)$ for $N = -2+$, $2+$, 3 , and $4+$ at $B/B_0 = 0.023$ as a function of V/t'_b in Fig. 4. In this case the highest peak is given by $N = 3$ or $2+$, which means that a negative quantum Hall effect is not stabilized. It is not the case in $(\text{TMTSF})_2\text{ClO}_4$ and $(\text{TMTSF})_2\text{PF}_6$. We denote this choice of

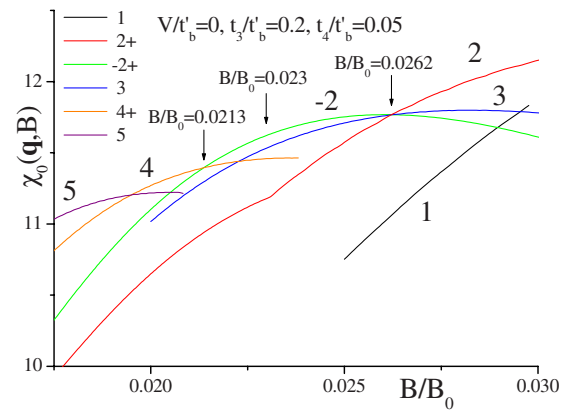


FIG. 7. (Color online) The maximum of $\chi_0(\mathbf{q}, B)$ for the non-perturbative calculation for $V/t'_b = 0$ and $t_3/t'_b = 0.2$, $t_4/t'_b = 0.05$.

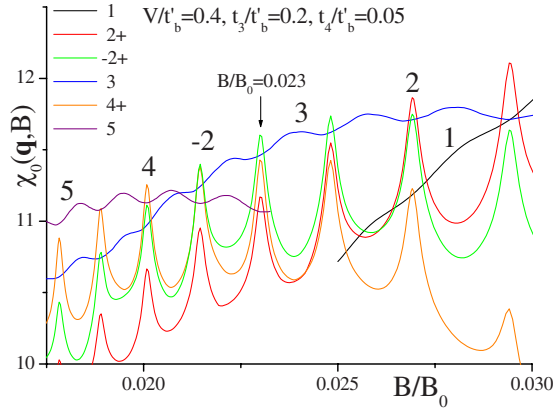


FIG. 8. (Color online) The maximum of $\chi_0(\mathbf{q}, B)$ for the non-perturbative calculation for $V/t'_b=0.4$ and $t_3/t'_b=0.2$, $t_4/t'_b=0.05$.

t_3/t'_b and t_4/t'_b as a triangle (\triangle) in the parameter plane of t_3/t'_b and t_4/t'_b as seen in Fig. 10.

The finite value of t_4 is necessary for the maximum of $\chi_0(\mathbf{q}, B)$ to be the absolute maximum at some B . We show the example of the parameter ($t_3/t'_b=0.2$ and $t_4/t'_b=0.02$) in Fig. 5. Taking this choice of the parameters t_3/t'_b and t_4/t'_b , we plot the maximum of $\chi_0(\mathbf{q}, B)$ for $N=-2+$, $2+$, 3 , and $4+$ at $B/B_0=0.023$ as a function of V in Fig. 6. The maximum of $\chi_0(\mathbf{q}, B)$ for $N=-2$ is the absolute maximum when $0.2 \leq V/t'_b \leq 0.8$ and $B \sim 9$ T. We think this choice of t_3/t'_b and t_4/t'_b is a candidate for $(\text{TMTSF})_2\text{ClO}_4$ because the negative N phase is realized only when the cooling rate is slow,⁴⁵ which is interpreted as a large V . We depict it by a filled blue circle (\bullet) in the parameter plane of t_3/t'_b and t_4/t'_b as seen in Fig. 10.

If we take $t_3/t'_b=0.2$ and $t_4/t'_b=0.05$, the maximum of $\chi_0(\mathbf{q}, B)$ for $N=-2$ is the absolute maximum at $0.0213 \leq B/B_0 \leq 0.0262$ even when $V=0$, as seen in Fig. 7. In these parameters of t_3/t'_b and t_4/t'_b the maximum of $\chi_0(\mathbf{q}, B)$ for $N=-2$ is still the absolute maximum at $B/B_0=0.023$ when $V/t'_b=0.4$, as seen in Fig. 8. The maximum of $\chi_0(\mathbf{q}, B)$ for $N=-2+$, $2+$, 3 , and $4+$ at $B/B_0=0.023$ is plotted as a function of V/t'_b in Fig. 9. The maximum of $\chi_0(\mathbf{q}, B)$ for $N=-2$ is the largest at $0 \leq V/t'_b \leq 1.0$. With these parameters of t_3/t'_b

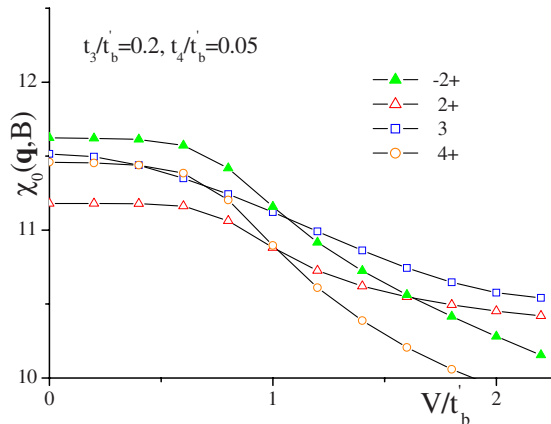


FIG. 9. (Color online) The maximum of $\chi_0(\mathbf{q}, B)$ at $B/B_0=0.023$ as a function of V/t'_b .

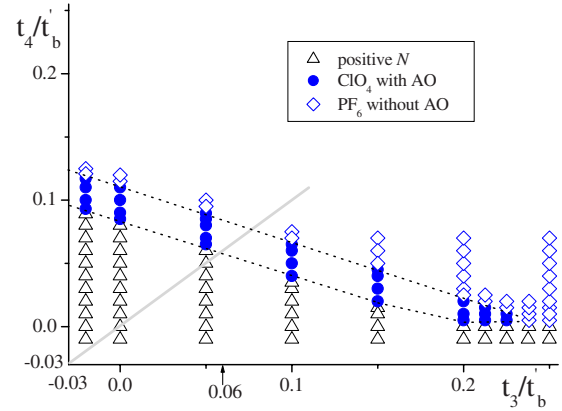


FIG. 10. (Color online) The phase diagram in t_3 and t_4 plain. Dotted lines are for the eye guide. A thick gray solid line represents $t_3=t_4$.

and t_4/t'_b , the negative N phase is realized without the anion ordering, which is the case in $(\text{TMTSF})_2\text{PF}_6$. We denote it by a blue open diamond (\diamond) in the parameter plane of t_3/t'_b and t_4/t'_b as seen in Fig. 10. Taking various values of parameters

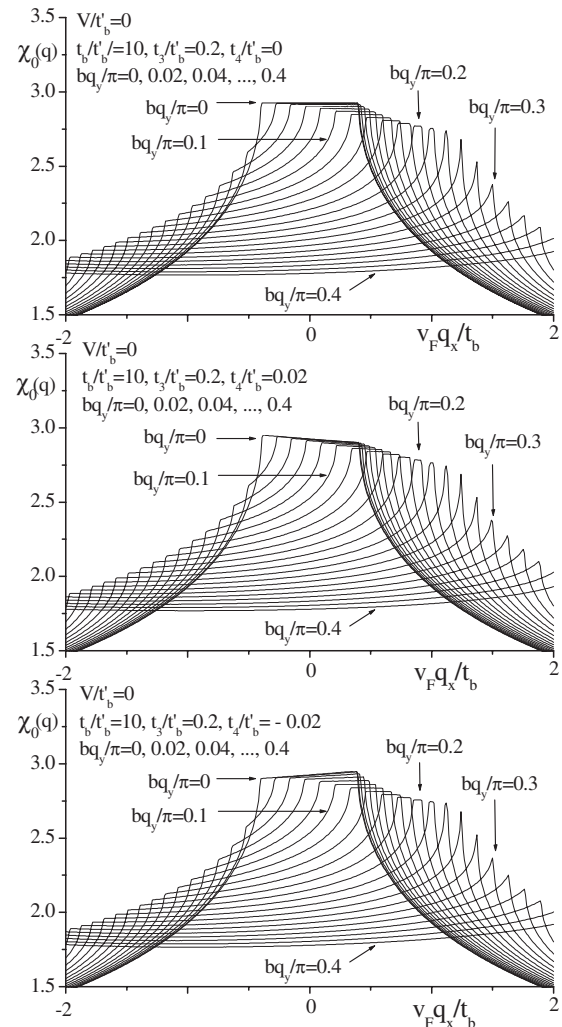


FIG. 11. $\chi_0(\mathbf{q})$ at $B=0$ from $t_4/t'_b=0$ to $t_4/t'_b=0.02$ and $t_4/t'_b=-0.02$ when $V=0$.

t_3/t'_b and t_4/t'_b , we obtain Fig. 10. In order to obtain a negative phase, t_4 must be a nonzero positive value. In fact, the susceptibility at $B=0$ [$\chi_0(\mathbf{q},0)=\chi_0(\mathbf{q})$] is maximized at $q_x > 0$ ($q_x < 0$) when t_4 is negative (positive), which is shown in Fig. 11.

IV. CONCLUSION

We obtain the possible parameter region of t_3/t'_b and t_4/t'_b for $(\text{TMTSF})_2\text{PF}_6$ and $(\text{TMTSF})_2\text{ClO}_4$. The negative N phase in FISDW is observed in $(\text{TMTSF})_2\text{PF}_6$ in which the centrosymmetric anions give no periodic potential ($V=0$). In this case t_3/t'_b and t_4/t'_b should be in the regions marked by the blue diamonds in Fig. 10. On the other hand, the negative N phase in $(\text{TMTSF})_2\text{ClO}_4$ is observed only when the cooling rate is slow. Thus the parameters t_3/t'_b and t_4/t'_b should be in the region denoted by filled blue circles in Fig. 10. It is natural to assume $t_4 \leq t_3$. Then we conclude that the parameters for $(\text{TMTSF})_2\text{ClO}_4$ are in the region enclosed by dotted lines and a gray line in Fig. 10, which are $0.06 \leq t_3/t'_b \leq 0.23$ and $0 \leq t_4/t'_b \leq 0.08$. It is noted that t_3/t'_b and t_4/t'_b for $(\text{TMTSF})_2\text{ClO}_4$ are smaller than those for $(\text{TMTSF})_2\text{PF}_6$.

We studied the effects of the parameters, t_3/t'_b , t_4/t'_b , and V on the stability of the negative N phase in FISDW. The

parameters, t_3/t'_b , t_4/t'_b , and V may give a key to explain the unexpected periodic oscillation⁴⁶ in the FISDW with sign reversal of R_{xy} above $B \simeq 26$ T.

Furthermore, these parameters may affect the superconductivity especially in the FFLO state,^{41,42} where the nesting of the Fermi surface plays an essential role. The upper critical field exceeds the Pauli-Clogston limit in $(\text{TMTSF})_2\text{PF}_6$ (Ref. 65) and $(\text{TMTSF})_2\text{ClO}_4$.⁶⁶ The superconductivity in $(\text{TMTSF})_2\text{PF}_6$ is considered to be spin triplet from the absence of the change in the ⁷⁷Se Knight shift⁶⁷ while the spin-singlet superconductivity in $(\text{TMTSF})_2\text{ClO}_4$ is suggested from the change in Knight shift.⁶⁸ The pairing symmetry of $(\text{TMTSF})_2X$ is also still controversial. Both possibilities have been asserted theoretically.^{23,69–80} Many authors^{69–80} have not taken account of t_3 , t_4 , and V in the theoretical study while a few authors have studied with V and t_3 in Refs. 75 and 80, respectively. Since we have obtained that the upper critical field for the spin-singlet superconductivity is enhanced by taking account of the higher harmonics up to t_3 ,²³ we expect that the theory including these effects makes clear the unexplained results such as the critical temperature with the anomalous in-plane anisotropy^{39,40} in which the realization of two kinds of the FFLO superconductivity^{41,42} is suggested.

¹T. Ishiguro, K. Yamaji, and G. Saito, *Organic Superconductors*, 2nd ed. (Springer-Verlag, Berlin, 1998).

²J. F. Kwak, J. E. Schirber, R. L. Greene, and E. M. Engler, *Phys. Rev. Lett.* **46**, 1296 (1981).

³P. M. Chaikin, M. Y. Choi, J. F. Kwak, J. S. Brooks, K. P. Martin, M. J. Naughton, E. M. Engler, and R. L. Greene, *Phys. Rev. Lett.* **51**, 2333 (1983).

⁴M. Ribault, D. Jerome, J. Tuchendler, C. Weyl, and K. Bechgaard, *J. Phys. (Paris)*, Lett. **44**, L953 (1983).

⁵M. J. Naughton, J. S. Brooks, L. Y. Chiang, R. V. Chamberlin, and P. M. Chaikin, *Phys. Rev. Lett.* **55**, 969 (1985).

⁶M. J. Naughton, R. V. Chamberlin, X. Yan, S. Y. Hsu, L. Y. Chiang, M. Ya. Azbel, and P. M. Chaikin, *Phys. Rev. Lett.* **61**, 621 (1988).

⁷W. Kang, S. T. Hannahs, and P. M. Chaikin, *Phys. Rev. Lett.* **70**, 3091 (1993).

⁸M. Ribault, *Mol. Cryst. Liq. Cryst.* **119**, 91 (1985).

⁹U. M. Scheven, E. I. Chashechkina, E. Lee, and P. M. Chaikin, *Phys. Rev. B* **52**, 3484 (1995).

¹⁰J. R. Cooper, W. Kang, P. Auban, G. Montambaux, D. Jerome, and K. Bechgaard, *Phys. Rev. Lett.* **63**, 1984 (1989).

¹¹S. T. Hannahs, J. S. Brooks, W. Kang, L. Y. Chiang, and P. M. Chaikin, *Phys. Rev. Lett.* **63**, 1988 (1989).

¹²L. Balicas, G. Kriza, and F. I. B. Williams, *Phys. Rev. Lett.* **75**, 2000 (1995).

¹³W. Kang, J. R. Cooper, and D. Jerome, *Phys. Rev. B* **43**, 11467 (1991).

¹⁴S. Uji, C. Terakura, M. Takashita, T. Terashima, H. Aoki, J. S. Brooks, S. Tanaka, S. Maki, J. Yamada, and S. Nakatsuji, *Phys. Rev. B* **60**, 1650 (1999).

¹⁵D. Jerome, A. Mazaud, M. Ribault, and K. Bechgaard, *J. Phys.*

(France) Lett. **41**, 95 (1980).

¹⁶K. Bechgaard, K. Carneiro, M. Olsen, F. B. Rasmussen, and C. S. Jacobsen, *Phys. Rev. Lett.* **46**, 852 (1981).

¹⁷W. Kang, T. Osada, Y. J. Jo, and H. Kang, *Phys. Rev. Lett.* **99**, 017002 (2007).

¹⁸K. Yamaji, *J. Phys. Soc. Jpn.* **55**, 860 (1986).

¹⁹P. M. Grant, *J. Phys. Colloq.* **44**, C3-847 (1983).

²⁰L. Ducasse, M. Abderrabba, J. Hoarau, M. Pesquer, B. Gallois, and J. Gaultier, *J. Phys. C* **19**, 3805 (1986).

²¹D. Zanchi and G. Montambaux, *Phys. Rev. Lett.* **77**, 366 (1996).

²²N. Dupuis and V. M. Yakovenko, *Phys. Rev. Lett.* **80**, 3618 (1998).

²³M. Miyazaki, K. Kishigi, and Y. Hasegawa, *J. Phys. Soc. Jpn.* **68**, 3794 (1999).

²⁴L. P. Gor'kov and A. G. Lebed', *J. Phys. (Paris)*, Lett. **45**, 433 (1984).

²⁵G. Montambaux, M. Heritier, and P. Lederer, *Phys. Rev. Lett.* **55**, 2078 (1985).

²⁶K. Yamaji, *J. Phys. Soc. Jpn.* **54**, 1034 (1985).

²⁷A. G. Lebed', *Sov. Phys. JETP* **62**, 595 (1985).

²⁸K. Maki, *Phys. Rev. B* **33**, 4826 (1986).

²⁹A. Virosztek, L. Chen, and K. Maki, *Phys. Rev. B* **34**, 3371 (1986).

³⁰L. Chen and K. Maki, *Phys. Rev. B* **35**, 8462 (1987).

³¹K. Yamaji, *J. Phys. Soc. Jpn.* **56**, 1841 (1987).

³²K. Machida, Y. Hori, and M. Nakano, *Phys. Rev. Lett.* **70**, 61 (1993).

³³A. G. Lebed, *Phys. Rev. Lett.* **88**, 177001 (2002).

³⁴D. Poilblanc, G. Montambaux, M. Heritier, and P. Lederer, *Phys. Rev. Lett.* **58**, 270 (1987).

³⁵V. M. Yakovenko, *Phys. Rev. B* **43**, 11353 (1991).

- ³⁶K. Sengupta, Hyo-Jon Kwon, and V. M. Yakovenko, *Phys. Rev. Lett.* **86**, 1094 (2001).
- ³⁷K. Machida, Y. Hasegawa, M. Kohmoto, V. M. Yakovenko, Y. Hori, and K. Kishigi, *Phys. Rev. B* **50**, 921 (1994).
- ³⁸P. Lederer and C. M. Chaves, *Phys. Rev. B* **58**, 3302 (1998).
- ³⁹S. Yonezawa, S. Kusaba, Y. Maeno, P. Auban-Senzier, C. Pasquier, K. Bechgaard, and D. Jerome, *Phys. Rev. Lett.* **100**, 117002 (2008).
- ⁴⁰S. Yonezawa, S. Kusaba, Y. Maeno, P. Auban-Senzier, C. Pasquier, and D. Jerome, *J. Phys. Soc. Jpn.* **77**, 054712 (2008).
- ⁴¹P. Fulde and R. A. Ferrell, *Phys. Rev.* **135**, A550 (1964).
- ⁴²A. I. Larkin and Y. N. Ovchinnikov, *Sov. Phys. JETP* **20**, 762 (1965).
- ⁴³S. K. McKernan, S. T. Hannahs, U. M. Scheven, G. M. Danner, and P. M. Chaikin, *Phys. Rev. Lett.* **75**, 1630 (1995).
- ⁴⁴N. Matsunaga, A. Ayari, P. Monceau, A. Ishikawa, K. Nomura, M. Watanabe, J. Yamada, and S. Nakatsuji, *Phys. Rev. B* **66**, 024425 (2002).
- ⁴⁵N. Matsunaga, K. Hino, T. Ohta, K. Yamashita, K. Nomura, T. Sasaki, A. Ayari, P. Monceau, M. Watanabe, J. Yamada, and S. Nakatsuji, *J. Phys. IV* **131**, 269 (2005).
- ⁴⁶S. Uji, S. Yasuzuka, T. Konoike, K. Enomoto, J. Yamada, E. S. Choi, D. Graf, and J. S. Brooks, *Phys. Rev. Lett.* **94**, 077206 (2005).
- ⁴⁷K. Kishigi and Y. Hasegawa, *Phys. Rev. B* **75**, 245107 (2007).
- ⁴⁸Y. Hasegawa and K. Kishigi, *Phys. Rev. B* **78**, 045117 (2008).
- ⁴⁹A. G. Lebed, Heon-Ick Ha, and M. J. Naughton, *Phys. Rev. B* **71**, 132504 (2005).
- ⁵⁰H. Yoshino, S. Shodai, and K. Murata, *Synth. Met.* **133-134**, 55 (2003).
- ⁵¹K. Kishigi, K. Machida, and Y. Hasegawa, *J. Phys. Soc. Jpn.* **66**, 2969 (1997).
- ⁵²K. Kishigi, *J. Phys. Soc. Jpn.* **67**, 3825 (1998).
- ⁵³Y. Hasegawa, K. Kishigi, and M. Miyazaki, *J. Phys. Soc. Jpn.* **67**, 964 (1998).
- ⁵⁴M. Miyazaki, K. Kishigi, and Y. Hasegawa, *J. Phys. Soc. Jpn.* **68**, 313 (1999).
- ⁵⁵L. P. Gor'kov and A. G. Lebed, *Phys. Rev. B* **51**, 3285 (1995).
- ⁵⁶K. Sengupta and N. Dupuis, *Phys. Rev. B* **65**, 035108 (2001).
- ⁵⁷D. Zanchi and A. Bjelis, *Europhys. Lett.* **56**, 596 (2001).
- ⁵⁸D. Radic, A. Bjelis, and D. Zanchi, *Phys. Rev. B* **69**, 014411 (2004).
- ⁵⁹S. Haddad, S. Charfi-Kaddour, C. Nickel, M. Heritier, and R. Bennaceur, *Phys. Rev. Lett.* **89**, 087001 (2002).
- ⁶⁰S. Haddad, S. Charfi-Kaddour, M. Heritier, and R. Bennaceur, *Phys. Rev. B* **72**, 085104 (2005).
- ⁶¹A. G. Lebed, *Phys. Rev. Lett.* **74**, 4903 (1995).
- ⁶²A. G. Lebed, *Phys. Rev. B* **55**, 1299 (1997).
- ⁶³T. Osada, S. Kagoshima, and N. Miura, *Phys. Rev. Lett.* **69**, 1117 (1992).
- ⁶⁴A. G. Lebed and P. Bak, *Phys. Rev. B* **40**, 11433 (1989).
- ⁶⁵I. J. Lee, M. J. Naughton, G. M. Danner, and P. M. Chaikin, *Phys. Rev. Lett.* **78**, 3555 (1997).
- ⁶⁶J. I. Oh and M. J. Naughton, *Phys. Rev. Lett.* **92**, 067001 (2004).
- ⁶⁷I. J. Lee, S. E. Brown, W. G. Clark, M. J. Strouse, M. J. Naughton, W. Kang, and P. M. Chaikin, *Phys. Rev. Lett.* **88**, 017004 (2001).
- ⁶⁸J. Shinagawa, Y. Kurosaki, F. Zhang, C. Parker, S. E. Brown, D. Jerome, K. Bechgaard, and J. B. Christensen, *Phys. Rev. Lett.* **98**, 147002 (2007).
- ⁶⁹X. Huang and K. Maki, *Phys. Rev. B* **39**, 6459 (1989).
- ⁷⁰A. G. Lebed, *Phys. Rev. B* **59**, R721 (1999).
- ⁷¹A. G. Lebed, K. Machida, and M. Ozaki, *Phys. Rev. B* **62**, R795 (2000).
- ⁷²A. G. Lebed, *JETP Lett.* **44**, 114 (1986).
- ⁷³N. Dupuis and G. Montambaux, *Phys. Rev. B* **49**, 8993 (1994).
- ⁷⁴Y. Hasegawa and M. Miyazaki, *J. Phys. Soc. Jpn.* **65**, 1028 (1996).
- ⁷⁵H. Shimahara, *Phys. Rev. B* **61**, R14936 (2000).
- ⁷⁶C. D. Vaccarella and C. A. R. Sa de Melo, *Phys. Rev. B* **63**, 180505(R) (2001).
- ⁷⁷K. Kuroki, R. Arita, and H. Aoki, *Phys. Rev. B* **63**, 094509 (2001).
- ⁷⁸H. Aizawa, K. Kuroki, T. Yokoyama, and Y. Tanaka, *Phys. Rev. Lett.* **102**, 016403 (2009).
- ⁷⁹N. Belmechri, G. Abramovici, and M. Heritier, *EPL* **82**, 47009 (2008).
- ⁸⁰P. D. Grigoriev, *Phys. Rev. B* **77**, 224508 (2008).